Title
ANGULAR DISTRIBUTIONS OF GAMMA RAYS PRODUCED IN REACTIONS WITH HEAVT IONS

Authors
Newton, J.O.
Stephens, F.S.
Diamond, R.M.
et al.

Publication Date
1966-10-17

UCRL-17204

University of California

Ernest O. Lawrence Radiation Laboratory

ANGULAR DISTRIBUTIONS OF GAMMA RAYS PRODUCED IN REACTIONS WITH HEAVY IONS

Berkeley, California

DISCLAIMER

To be submitted to Nuclear Physics

UCRL-17204
Preprint

UNIVERSITY OF CALIFORNIA

Lawrence Radiation Laboratory
Berkeley, California

AEC Contract No. W-7405-eng-48

ANGULAR DISTRIBUTIONS OF GAMMA RAYS PRODUCED IN REACTIONS WITH HEAVY IONS

J. O. Newton, F. S. Stephens, R. M. Diamond, K. Kotajima and E. Matthias

October 17, 1966

ANGULAR DISTRIBUTIONS OF GAMMA RAYS PRODUCED IN REACTIONS WITH HEAVY IONS

J. O. Newton, F. S. Stephens, R. M. Diamond, K. Kotajima* and E. Matthias

Lawrence Radiation Laboratory
University of California
Berkeley, California

October 17, 1966

Abstract

Angular distributions of the stretched E2 gamma-ray transitions cascading from rotational or vibrational states, populated by heavy-ion, xn reactions, have been measured. The reactions were induced by ^{4}He, ^{11}B, ^{14}N and ^{19}F ions on targets in the mass range from 159 to 186. In one case the variation of anisotropy with bombarding energy was measured. Large anisotropies were observed indicating the strong alignements of the decaying states. The problems involved in a theoretical calculation of the alignements are discussed. The implications of the strong angular distributions for nuclear structure measurements with these reactions are considered.

*Present address: Yale University, New Haven, Connecticut, USA.

alignment of their angular momenta in the plane perpendicular to the beam direction. The rapid subsequent decay of these highly excited compound systems, by neutron and gamma emission, leaves the angular momentum vector of the populated rotational or vibrational state still strongly aligned, thus causing considerable anisotropies in the angular distributions of the cascading gamma rays deexciting this state.

Whilst the investigations of these angular distributions are of value from the point of view of understanding the reaction mechanism, it is probably true at present that their main interest lies in the field of nuclear spectroscopy. This is because a detailed study of the reaction mechanism involves many complicated features, such as level densities, which at present are not fully understood. For nuclear spectroscopy, the angular distributions provide additional, much needed data on which to base the interpretation of the observed radiations. So far most of the studies of gamma rays and conversion electrons, following xn reactions, have been interpreted mainly on the basis of the energy systematics of collective states. In a previous paper[9]) we have discussed explicitly how one can use this feature of the reaction in spectroscopic studies.

The anisotropy of the radiation, if not taken into account, can introduce large errors in the determination of the conversion coefficients. If the angular distribution of the gamma rays is given by

$$W(\theta) = 1 + A_2P_2(\cos\theta) + A_4P_4(\cos\theta),$$

then the angular distribution of the conversion electrons is

$$W(\theta) = 1 + b_2A_2P_2(\cos\theta) + b_4A_4P_4(\cos\theta).$$

The particle parameters b_2 are tabulated for some cases by Band et al.[10]) and the higher coefficients can be obtained from the b_2 with the aid of recurrence formulae[11]). The particle parameters vary considerably in magnitude from one multipolarity to another and may even change sign (see table 1). Significant variations also occur for conversion of a given transition in different atomic shells, moreover all of the coefficients vary with energy. Therefore, to obtain reliable measurements of conversion coefficients it is most desirable to measure the angular distributions of both the gamma rays and the conversion electrons. When it is not possible to make such simultaneous measurements of both angular distributions, the best procedure is to make both gamma and conversion electron measurements at an angle of 54° to the beam direction, this being the angle where $P_2(\cos\theta)$ term is zero. Clearly, even to obtain accurately the gamma ray or conversion electron relative intensities, one must take account of these angular anisotropies.

2. Experimental Method

The beams of heavy ions were produced by the Lawrence Radiation Laboratory Heavy-Ion Accelerator. The accelerator gave heavy-ion beams of various energies, with up to 20% duty cycle. The energies were measured by scattering the beam from a thin gold foil into a Si solid state counter. This counter was calibrated at the full energy of the accelerator (10.4 MeV/nucleon) and the interpolation to the lower energies was done by the means of a pulse generator. The accuracy of this method is expected to be within ±2%.

The target chamber was essentially a vertical, aluminum cylinder of 8 cm diameter and 0.16 cm wall thickness. The targets were of sufficient thickness to stop the beam completely and were accurately mounted on the axis of the cylinder at 45° to the beam direction. For beams of ^{11}B and heavier ions, the targets were self supporting foils, having thicknesses of the order of 80 mg/cm^2. The ^4He beams had considerably greater ranges than those of the heavier ions, so for the ^4He induced reactions the targets were about 50 mg/cm^2 in thickness, mounted on 150 mg/cm^2 thick lead backings. The beams were collimated by two lead apertures, placed 10 cm apart, the final one being 10 cm from the target. The beam could be focussed with a quadrupole lens and typically about one sixth of the beam hit the collimators and five sixths hit the target. The diameter of the beam spot on the target was 5 mm. The collimators were shielded with lead and we have found that the background arising from the collimators was negligible compared to the yield from the target.

The detectors were solid state counters of the Ge-Li type, with dimensions of 6 cm^2 by 8 mm. A typical width at half maximum for a 660 keV gamma ray incident on these counters was 5 keV. The detectors could be accurately rotated about the axis of the target chamber. The counter to target distance was in range of ten to fifteen cms. One detector, fixed at 90° to the beam direction, was used as a monitor. In some measurements two moveable detectors were used and in others only one.

At least two measurements were made at each angle. In addition to taking measurements of the spectra during the beam pulses (typically 5 msec in length), we took measurements between the beam pulses, so that any corrections for induced radioactivity in the target could be made. In all cases this correction turned out to be of negligible importance. Corrections for counting loss in the pulse height analysers were made by counting the pulses accepted by the analysers and also counting, with fast scalers, all those pulses which were applied to the analysers in the same range of pulse heights. The difference between these two counting rates gave the counting loss, which was kept in all cases below 10%.

Normalisation of the counts in the movable counters was achieved by using the counts in the monitor counter. This normalisation was done in two ways. In some of the bombardments a very intense peak from Coulomb excitation, either in the target or in the projectiles, was present and in these cases this peak was used for the normalisation. Where such a peak was not pronounced we used the total counts in a certain energy region for normalisation. This procedure is obviously more open to error than the first one, in that it is less easy to be sure that there is no contribution to the monitor spectrum from, for example, radiation from the collimators. However, we were able to check, in the cases where there was a Coulomb excitation peak, that this total count was always proportional to the counts in the Coulomb excitation peak to an accuracy of about 0.75%. Furthermore in the cases where there was no strong Coulomb excitation peak, we always checked our normalisation with the total count to a normalisation with a reaction peak to make sure that there were no gross errors arising from this procedure. No discrepancies inconsistent with the expected statistical errors were found. Therefore, we felt safe to use this method of normalisation, provided that we allowed an error of ±1%. This error was always much greater than that from counting statistics in the monitor. The reason for doing this, rather than normalising directly on one of the reaction peaks, was simply the greater statistical accuracy achieved.

In order to obtain the angular distribution from the normalized counts it was necessary to correct for any possible misalignement between the axis of rotation of the counters and the beam spot on the target, as well as for any attenuation of the gamma rays by the target material. The alignement was checked by measuring the angular distribution of the gamma rays from the 27 msec ^{199}Tl isomer[12]), taken between beam bursts. These 382 keV gamma rays, would be expected to have an isotropic angular distribution, because of the long lifetime of the isomeric state. The target attenuation was checked by measuring the angular distribution of the gamma rays from various gamma ray sources, which were placed against the target in the position of the beam spot. The position of the beam spot was determined by radio-autograph of the alpha activity induced in a gold target. It was found that no correction for misalignement was required and that only the gamma rays of lowest energy required correction for attenuation. This correction amounted to 10% in the worst case of the heavy ion induced reactions and 25% in the worst case of the ^{4}He induced reactions, where thicker targets were required. The final angular distributions were corrected for the attenuation due to the finite solid angles of the detectors[13]).

The target chamber that we used required a thick target which would completely stop the beam of heavy ions. Therefore we were limited to studying the reactions which occurred with incident energies only a little above the Coulomb potential barrier for each particular reaction. Higher ion energies would produce a variety of reactions and a high background. In each case the bombarding energy was chosen so that the yield from the desired reaction was dominant. The measurements which we report on here are therefore only concerned with (4n) and (5n) reactions for heavy ions and 2n reactions for ^{4}He ions.

Although it would be interesting to study reactions in which more neutrons are emitted and larger angular momenta brought into the compound systems by the higher energy projectiles, we made this choice of target chamber in order to be able to cover all angles of observation from 0° to 90°. The use of a thin target would have required a flight tube to allow the beam, which had passed through the target, to reach a suitably shielded Faraday cup. With our present Ge-Li detector mountings this would have severely restricted observations at the forward angles and would consequently have made the measurements, particularly of the coefficients of the $P_4(\cos\theta)$ terms, must less precise.

The assignements of many of the transitions in the rotational nuclei formed in these reactions have been made previously by Stephens et al.[2]), who observed the conversion electrons from the decay of the corresponding states. The transitions in the vibrational nuclei have been assigned in the work of Burde et al.[5]), where both conversion electron spectra and gamma ray spectra were reported. Most of the Ge(Li) gamma spectra for rotational nuclei in this paper are the first ones to have been obtained for these particular reactions. These measurements also give new information on the ground state rotational bands of ^{184}Os, ^{186}Os and ^{188}Os. The spectroscopic aspects of these data are discussed in a companion paper[14]).

3. Results

The ten reactions which we studied are listed in table 2. Typical spectra for the gamma rays of these reactions are shown in figs. 1-3. The spectra from the ^{182}W, ^{184}W, $^{186}W(^{4}He,2n)$ reactions are presented in fig. 1 in the following paper[14]. Some of the angular distributions are shown in fig. 4.

For each reaction the normalized intensities of the gamma rays at all of the angles of observation were fitted, by means of a least squares computer program, to a function of the form $W(\theta) = A_0 + A_2P_2(\cos\theta) + A_4P_4(\cos\theta)$. For any particular reaction the coefficients A_0 give the relative intensities of the gamma rays, after correction for counter efficiency has been made. The relative counting efficiencies were obtained using the accurately known relative gamma ray intensities in the decays of ^{177m}Lu [15], ^{22}Na [16] and ^{207}Bi [17]. In table 2 the coefficients A_2 and A_4, corrected for finite geometry, are given for all of the angular distributions. The relative transition intensities for each reaction are also shown in table 2. In each case the intensity of the $4+ \rightarrow 2+$ transition was taken to be unity. The transition intensities were obtained from the gamma ray intensities by correcting them for internal conversion. Since all of the transitions, with which we are concerned here, are pure E2 transitions, the correction is easy to make from the published tables of internal conversion coefficients[18] and should involve little error. We assumed that the ratio of $M + N + \cdots$ shell conversion to L shell conversion was 0.33. The errors on the relative intensities are estimated to be about $\pm 10\%$.

In the case of $^{184}W(^{4}He,2n)^{186}Os$ reaction we studied the variation of anisotropy with bombarding energy. A thin target arrangement together with two detectors at 90° and 45° to the beam direction was employed. The target consisted of a fine powder of ^{184}W deposited on 0.0006 cm mylar. It was about 4 MeV thick to ^{4}He ions. The ratios of the counts taken in each detector for a number of transitions were obtained as a function of bombarding energy and the results are shown in fig. 5. It can be seen that, within the accuracy of the measurement, there is no change of anisotropy with bombarding energy.

4. Discussion

4.1. THE ANGULAR DISTRIBUTIONS

The pronounced angular distributions of the de-excitation gamma rays observed in heavy-ion, xn reactions are a consequence of the fact that a reaction of this type proceeds mainly through a compound nucleus mechanism[19,20]) and that the incoming projectile brings in orbital angular momentum in the m = 0 substate only, taking the beam axis as the axis of quantisation[21]). Heavy ions bring into the compound system large amounts of orbital angular momentum, average values of twenty to fifty are common, so that, even if the target and projectiles have spins, the compound nucleus will, on the average, have its angular momentum vector strongly aligned. Several neutrons may be evaporated from the compound nucleus before a particle stable state, which can decay by gamma emission, is formed and several gamma rays may then be emitted before one of the rotational states of the final nucleus is reached[22,23]). The angular momentum taken away in any one of these steps is small, the average being about two[22]). Moreover, the angular momentum vectors of the individual events will be distributed in approximately random directions, so that the angular momentum of the rotational state will still be strongly aligned, though less so than that of the compound nucleus. This aligned rotational state will give rise to a cascade of stretched

E2 transition, leading finally to the ground state. As is well known all of these gamma rays will have the same angular distribution, the anisotropy of which will depend on the degree of alignement and the spin of the initial state [21].

Whilst it is easy to see why the pronounced angular distributions are obtained, it is not easy to give a quantitative explaination of the results. We shall only point out here some of the things which will have to be taken into account in such an analysis and draw a few qualitative conclusions. The first factor, which must be evaluated, is the angular momentum distribution of the compound system. This involves the orbital angular momenta brought in by the projectiles and the spins of the target and projectile. The incoming projectiles of higher orbital angular momenta interact with the surface region of the target nucleus. They tend to induce direct reactions rather than compound nucleus formation,[24,25]. This effect, which can only be roughly estimated at present, must be taken into account in assessing the distribution of the orbital angular momenta contributing to compound nucleus formation. The distribution of angular momenta in the compound system will differ from this if the target and projectile have non-zero spins. When heavy ions with large average angular momenta are brought into the system this difference will be quite small, but in case of helium or lighter ions the difference may be important.

The distribution of the z component of angular momentum $|m|$ in the compound system depends only on target and projectile spins, which are randomly oriented, since the incoming orbital angular momentum has m=0. This distribution of m is the same for all states and is easily calculated. The maximum value for $|m|$, which can occur in a given case, is simply the sum of these two spins and rarely exceedes five. The states in the compound system, having angular momentum greater than 10, will therefore always be strongly aligned; those having small angular momenta may not be if the target and projectile have large spins. Since the partial cross section for the incident angular momentum ℓ is approximately proportional to $(2\ell + 1)$ and, for a typical heavy ion reaction, ℓ may go up to twenty or more, it is clear that most of the states in the coumpound nucleus will be strongly aligned, even when the target and projectile have large spins. This may not be true for ^{4}He induced reactions, where the maximum value of ℓ is much lower.

The next step would be to obtain the angular momenta alignements of the particle stable states, which are reached after the cascade of evaporated neutrons. The alignements will be affected most at this stage, since it is generally supposed that the average value of J does not change by more than a few units in the cascade[26,27]. It must however be remarked that the theoretical basis for this assumption does not appear to be strong at present. In order to get an idea of the angular momentum distributions in the final nucleus, after the neutron cascade, some of these were calculated with a program obtained from Sikkeland and are shown in fig. 6. This program took into account the surface reactions in a rough way and necessarily made some approximations, but is unlikely to be grossly in error.

The alignements of the particle stable states depend on two factors. The first of these is the relative orientation of the angular momentum vectors of the outgoing neutrons to the angular momentum vector of the initial state. There are two extreme cases of this. One is when all the neutron transitions are stretched, in which case there is little effect on the alignement. The other is when there is no correlation between the directions of all the vectors. The true situation lies somewhere in between and to evaluate it one needs to know how the level densities in the intermediate and final nuclei vary with energy and angular momentum. Up to this time there is no adequate treatment of level density. The other factor on which the alignement depends is the absolute magnitude of the angular momentum carried away by each neutron. In fig. 7 we illustrate the especially simple case of a ^{4}He,2n reaction. A typical spectrum for the energy of the outgoing neutrons is shown together with an indication of the average angular momentum carried away by neutrons in different regions of this spectrum. The higher energy neutrons carry away more angular momentum and therefore cause more misalignement than do those of lower energy. Thus the alignement of the particle stable states in the final nucleus depends on the excitation energy in that nucleus, the states of lower energy being less aligned than those of higher energy. This effect may be of greater importance when more than two neutrons are emitted. Account must also be taken of the fact that sometimes charged particle emission may be more probable than either neutron or gamma ray emission. This situation will most probably occur in the last stage of particle emission from states of very high angular momentum. There may be no states of similar angular momentum in the residual nucleus to which neutron decay can occur, so that neutron emission will be severely inhibited by the centrifugal barrier. Alpha decay, which is probably the most likely to occur, is not so severely slowed down by the centrifugal barrier and moreover alpha particles are less strongly bound, to the extent of about 13 MeV, than are neutrons.

Finally, the effects on the alignement due to the gamma ray cascade, before the rotational state is reached, have to be evaluated. Again, this depends on details of the level density and probably, in the last stages of the cascade, on details peculiar to that particular final nucleus. Even the matrix elements for electromagnetic decay in the statistical region are not understood at present[28]), though what little experimental evidence there is suggests that the decay is predominantly quadrupole rather than dipole[22]).

At the present stage of our knowledge of all the factors which would have to come into such a calculation, it seems to us not worth while to attempt one, since there are just too many unknowns which cannot be easily separated. Perhaps an exception to this is the case of an ^{4}He,2n reaction very close to threshold. Rasmussen and Sugihara[29]) have pointed out that this would involve only relatively low energy states in the final nucleus, which have some chance of being understood and one might, in this case, learn something useful. Sakai et al.[4]) have, however, attempted a calculation of the angular distributions of the gamma rays from p,2n reactions.

We shall now make some observations on our results from a much more restricted point of view than that above. From our data we obtain only two parameters. These are the values of A_2 and A_4, the coefficients of the $P_2(\cos\theta)$ and the $P_4(\cos\theta)$ terms in the angular distributions. For a state of spin J there are (J + 1) magnetic substates with different values of $|m|$, m being the z component of J. Thus our two parameters will not be sufficient to define the distribution in $|m|$, which determines the angular distribution of the gamma rays from the state J. There will in general be many substate distributions which will result in the same angular distribution. We can however consider some physically plausible distribution and see whether this corresponds in any way to the experimental observations. The most obvious, but not necessarily the most correct, is the Gaussian distribution. It turns out, for Gaussian distributions of the substate populations, that to a good degree of approximation one can draw a curve relating A_2 to A_4, which will apply whatever the initial spin of the state. (We are referring here only to the stretched E2 transitions in the ground state band of an even nucleus). A point on this curve will refer to a Gaussian distribution of a particular width, for an initial state of a particular spin. For a state of different spin the width will be different. In order to test our hypothesis of a Gaussian distribution of substates we simply have to plot all of our experimental data with A_2 and A_4 as co-ordinates and see whether the points lie about the curve derived on our assumption. Such a plot is shown in fig. 8. It can be seen that on the whole the transitions originating from the high spin states are consistent with the curve, whereas those from the low spin states lie above it.

It is probably only sensible to expect to obtain a Gaussian distribution of substates provided that the particular state concerned is fed via a large number of routes, none of which is dominant. This is certainly not the case for the lower spin states of the rotational band, since most of their feeding comes from the next higher rotational state, but it may be roughly true for the highest rotational state seen. For a particular cascade the width of the distribution in $|m|$ will in fact get progressively smaller as one proceeds down the band by stretched E2 transitions, corresponding to an approximately constant misalignement of the angular momentum vector. We have no way of assessing theoretically the distributions in $|m|$ resulting from transitions which feed directly into the lower states of the band, compared to those which feed the highest band members seen. However, if we assume that the $|m|$ distributions are the same for all transitions feeding the ground band, then we obtain a result similar to that which we see in fig. 8, i.e. that the points for the lower rotational transitions should lie above the curve. A constant distribution for $|m|$ implies that the angular momentum vectors of the transitions feeding the rotational band are less aligned, the smaller the angular momentum of the state which they feed. This general feature is in fact all that is required to give a result of the desired form.

The $2 \rightarrow 0$ transitions have particularly small anisotropies in some cases. These small anisotropies cannot easily be explained as arising from the relatively weak feeding of the 2+ state via pathways other than from the 4+ rotational state. In all cases where this effect is seen, the transition energy is low, of the order of 100 to 150 keV. The explaination seems likely to be that the angular distributions are perturbed by extra nuclear fields[30]. The half lives of these states are of the order of 10^{-9} sec, which is a sufficiently long time for such effects to occur. The alpha-gamma angular correlations observed in the decay of even actinide elements, leading to the 2+ rotational states, are observed to be perturbed, even though the half lives in these cases are of the order of 2.10^{-10} sec. The attenuations observed in these alpha-decay cases are consistent with those expected for a static quadrupole interaction[30]. The characteristic of this type of interaction is that the $P_2(\cos\theta)$ term is attenuated more than the $P_4(\cos\theta)$ term for the $2 \rightarrow 0$ transition. Such an interaction would also appear to be consistent with our results here.

It is interesting to evaluate the width σ in the Gaussian approximation, which corresponds to the observed anisotropies of the highest rotational states which we see. The Gaussian distribution in m is given by

$$W(m) = (2\pi\sigma^2)^{-\frac{1}{2}} \; e^{\frac{-m^2}{2\sigma^2}} .$$

If we take the mean values of A_2 and A_4 for the $12 \rightarrow 10$ transitions from the $^{165}Ho + ^{11}B$ and $^{159}Tb + ^{14}N$ results, which appear to be rather similar, we obtain $A_2 = 0.37 \pm 0.035$ and $A_4 = -0.11 \pm 0.04$. These values are to be compared with the values for complete alignement of the 12+ state of $A_2 = 0.404$ and $A_4 = -0.16$. It can be seen that, at the 12+ state, the values in these two cases do not depart very much from those for complete alignement. They correspond to a width $\sigma = 2.3^{+0.6}_{-2.3}$. The angular distribution in the $^{159}Tb + ^{11}B$ reaction is less anisotropic and corresponds to $\sigma = 4.3 \pm 1$. In all of these cases however it is clear that the 12+ state is rather strongly aligned. The $^{165}Ho + ^{11}B$ reaction gives one of the largest anisotropies, even though the maximum channel spin of 5 in this case is the largest of any of the reactions which we have studied. To get an idea of the effect of the target and projectile spins in this reaction we have worked out the values of A_2 and A_4, assuming that the misalignement of the 12+ state arises only from this effect and that the state is fed only from the component of orbital angular momentum 12 in the incident beam. The values obtained are $A_2 = 0.358$ and $A_4 = -0.108$, which are very close to those measured. However this is an overestimate of the reduction of anisotropy from this effect, since most of the feeding of the 12+ state arises from incoming angular momenta greater than 12 (see fig. 6) in which case the target and projectile spins will tend to produce less misalignement to the 12+ state. This agrees with our previous qualitative conclusion that the reduction of anisotropy from the spins of the target and projectile is not a major effect in heavy ion induced reactions. It may however be an important effect in ^4He induced reactions were much less orbital angular momentum is brought in (See fig. 6). It is interesting to note that there is no obvious correlation between our measured anisotropies, and either the maximum channel spins of target and projectile, or the distributions of angular momenta brought into the final nuclei. It should be noted however that the channel spin in our ^{4}He induced reactions was zero in all cases.

It is possible to estimate a rough upper limit to the value of σ due to the neutron cascade. Rasmussen and Sugihara[29]) have pointed out that the cascade will give rise to an approximately one dimensional random walk in the projection m. Thus after n steps of average step length (projection) μ we will have, approximately, a Gaussian distribution in m of width $\mu . n^{1/2}$. For evaporation of 4 neutrons and an average step length of 1, we obtain a value of 2 for this width. An average step length of 1 corresponds to an average angular momentum of about 2 carried away by each neutron, assuming that there is no correlation between the directions of the angular momentum vectors of the outgoing neutrons and the beam direction. This value is of the same order of magnitude as the minimum observed values of σ at the 12+ state.

Although all of the observed anisotropies are large, there are significant variations from one case to another. There is no obvious reason why there should be significant variations in the alignements in the statistical phase of the reactions, i.e. when very many pathways leading to a particular state are open. It seems likely that the differences arise because there may be, in some cases, only a few important pathways in the last stages of the gamma ray cascades leading to the rotational states. In such a situation if one or more non-stretched transitions occur, significant reductions of the anisotropies will result. Since these final pathways will differ from one nucleus to another the anisotropies will also differ. It is easy to calculate the effect of a non-stretched transition on the angular distribution and some discussion of the effects arising from these in heavy ion-xn reactions is given in the paper of Rasmussen and Sugihara[29]). Although one will occasionally expect to see significant reductions in anisotropy from this effect, the reduction would normally be expected to be small. Such heavily fed non-stretched transitions probably can account for the observed variation of anisotropy from one case to another. We may also add that even if the distribution in m were Gaussian after the statistical phase of the reaction, it would not be after one or more non-stretched transitions via a limited number of pathways. Thus we must also expect deviations from the Gaussian line in our plot from this effect.

As an example of the important pathways which can occur in the last stages of the gamma ray cascade we show, in fig. 9, part of the level scheme of ^{186}Os, as obtained by Emery et al.[31]). The intensities of the gamma rays are those which we observed in the $^{184}W(^{4}He,2n)^{186}Os$ reaction. It is clear that in this case there are a number of strong transitions, both stretched and non-stretched, which feed the rotational states. These transitions will have an important effect on the final angular distributions from the rotational states. Other strong transitions, not shown in the figure, also occur. A large number of transitions, other than those of the ground state rotational bands, are also seen in the reactions $^{182}W(^{4}He,2n)^{184}Os$ and $^{186}W(^{4}He,2n)^{188}Os$, as can be seen from fig. 1 of the following paper[14]). These three reactions show more strong non-rotational transitions than are usually seen in even nuclei, almost certainly because the gamma vibrational states are especially low lying in this region. There are therefore more states of relatively high spin at low excitation than is usual, and these states collect a significant part of the total intensity.

The result of the $^{184}W(^{4}He,2n)^{186}Os$ experiment, where we measured the variation of anisotropy with bombarding energy, is rather surprising. Since the average angular momentum brought into the ^{186}Os nucleus varies from about 4.5, at the lowest energy, to 11, at the highest, one might naively have expected to see some change in anisotropy, but there was none within the errors of the measurements. Presumably this must arise from a cancellation of the various effects mentioned earlier. With only one result of this type we are not really able to say more than this.

In summary, our results have shown that pronounced angular distributions, corresponding to large and fairly uniform alignements of the angular momentum vectors of the decaying states, are seen in heavy-ion, xn reactions. These results can be understood in a qualitative, but not quantitative way at present. It seems likely to us that the angular distributions will not afford a very sensitive tool for studying the mechanism of the heavy-ion, xn reactions. However we do feel that they offer a very powerful tool in spectroscopic studies of the nuclei which can be formed in these reactions. In a previous publication[9]) we have demonstrated the power of this technique for assigning spins and multipolarities of transitions. We have also indicated the possibilities of using the strong alignements in studies of nuclear moments and hyperfine interactions.

Table 2

Observed angular distribution coefficients. The bombarding energy for each reaction is given in brackets underneath its title. The transition intensities I and energies E, in keV, are also given

Transition		2 →0	4→2	6→4	8→6	10→8	12→10	14→12
$^{182}W(^{4}He,2n)^{184}Os$	E	119.8	263.8	390.1	500.7	596.6		
	A_2	0.198±.015	0.275±.010	0.320±.015	0.320±.047	0.20±.1		
	$-A_4$	0.051±.020	0.074±.012	0.053±.017	0.133±0.51	0.06±.1		
(27 MeV)	I	1.43	1.00	0.54	0.23	0.11		
$^{184}W(^{4}He,2n)^{186}Os$	E	137.2	296.8	434.8	551.8			
	A_2	0.135±.012	0.209±.013	0.190±.051	0.22 ±.09			
	$-A_4$	0.027±.012	0.035±.013	0.058±.053	0.14 ±.09			
(27 MeV)	I	1.75	1.00	0.46	0.16			
$^{186}W(^{4}He,2n)^{188}Os$	E	155.0	322.9	461.9	573.8			
	A_2	0.145±.009	0.229±.010	0.276±.029	0.377±.088			
	$-A_4$	0.057±.010	0.045±.011	0.023±.032	0.038±.096			
(27 MeV)	I	1.81	1.00	0.43	0.13			
$^{159}Tb(^{11}B,4n)^{166}Yb$	E	101.8	227.9	337.4	430.0	506.8	567.8	602.7
	A_2	0.063±.009	0.210±.007	0.233±.010	0.242±.016	0.217±.017	0.261±.042	0.187±.072
(54 MeV)	$-A_4$	0.027±.012	0.061±.009	0.069±.013	0.073±.020	0.058±.022	0.054±.051	0.016±.089
	I	1.29	1.00	0.84	0.59	0.66	0.26	0.17
$^{165}Ho(^{11}B,4n)^{172}Hf$	E		213.4	319.1	408.8	483.6	543.1	588.6
	A_2		0.240±.006	0.325±.010	0.340±.016	0.368±.028	0.374±.047	0.380±.107
(54 MeV)	$-A_4$		0.062±.007	0.039±.012	0.049±.018	0.071±.029	0.077±.052	0.125±.12
	I		1.00	0.68	0.55	0.35	0.21	0.13
$^{181}Ta(^{11}B,4n)^{188}Pt$	E	265	404	512				
	A_2	0.216±.009	0.270±.013	0.187±.022				
(54 MeV)	$-A_4$	0.030±.011	0.044±.014	0.078±.025				
	I	1.19	1.00	0.73				

Table 2 (continued)

Transition		$2 \rightarrow 0$	$4 \rightarrow 2$	$6 \rightarrow 4$	$8 \rightarrow 6$	$10 \rightarrow 8$	$12 \rightarrow 10$	$14 \rightarrow 12$
$^{159}Tb(^{14}N,5n)^{168}Hf$	E	123.9	261.1	371.1	456.1	522.0	569.4	
(93 MeV)	A_2	0.151±.014	0.315±.014	0.330±.020	0.337±.023	0.344±.036	0.367±.051	
	$-A_4$	0.046±.018	0.080±.018	0.114±.027	0.131±.030	0.074±.046	0.148±.065	
	I	1.17	1.00	0.91	1.08	0.76	0.49	
$^{165}Ho(^{14}N,5n)^{174}W$	E		243.1	349.2	432.5	498.0		
(93 MeV)	A_2		0.253±.018	0.249±.023	0.284±.046	0.379±.061		
	$-A_4$		0.093±.020	0.072±.026	0.061±.052	0.085±.069		
	I		1.00	0.99	0.59	0.40		
$^{181}Ta(^{14}N,5n)^{190}Hg$	E	416	625	730				
(93 MeV)	A_2	0.263±.015	0.262±.016	0.249±.028				
	$-A_4$	0.071±.018	0.094±.020	0.068±.033				
	I	0.92	1.00	0.61				
$^{159}Tb(^{19}F,4n)^{174}W$	E	111.9	243.1	349.2	432.5			
(92 MeV)	A_2		0.206±.025	0.323±.035	0.305±.072			
	$-A_4$		0.030±.029	0.077±.039	0.050±.080			
	I		1.00	1.04	0.56			

Figure Captions

Fig. 1. Gamma ray spectra from the bombardment of ^{159}Tb, ^{165}Ho and ^{181}Ta with 54 MeV ^{11}B ions.

Fig. 2. Gamma ray spectra from the bombardment of ^{159}Tb, ^{165}Ho and ^{181}Ta with 93 MeV ^{14}N ions.

Fig. 3. Spectrum of the gamma rays from the bombardment of ^{159}Tb with 92 MeV ^{19}F ions.

Fig. 4. Angular distributions of the gamma rays from the reaction ^{165}Ho(^{11}B,4n)^{172}Hf. The solid lines are the least squares fits to the points (see text). Two measurements were made at each angle and the points have been displaced slightly to show this.

Fig. 5. The yield at 45° divided by the yield at 90° for various gamma rays from the reaction ^{184}W(^{4}He,2n)^{186}Os. The absolute value of the vertical scale has no significance.

Fig. 6. Calculated distributions of angular momenta for final nuclei, formed in various heavy-ion,xn reactions, before the emission of gamma radiation. The distributions are averaged over thick targets.

Fig. 7. Diagramatic illustration of a typical reaction where 27 MeV ^{4}He ions are incident on a rare earth target (A-4, Z-2) with a Q value for formation of the compound nucleus (A,Z) of -2.5 MeV. (A,Z) evaporates neutrons having a spectrum similar to that shown in the insert. The temperature of 2 MeV, corresponding to the spectrum shown, is a little high for (^{4}He,2n) reactions but typical for reactions where 4 or 5 neutrons are emitted. To the right of the spectrum is indicated the average angular momentum taken away by neutrons of different energies. Most of the states populated by neutron emission from

(A,Z) have energies above the neutron binding energy (NBE) in (A-1,Z) and will decay to (A-2,Z) with a similar neutron spectrum, where this is allowed by the energetics. A small fraction of the states of (A-2,Z), so formed, will also be neutron unstable and may decay to (A-3,Z).

Fig. 8. The coefficients A_2 are plotted against A_4 (see text) for a number of rotational or vibrational gamma rays observed as the last step of a number of heavy-ion,xn reactions. Some $2\rightarrow 0$ transitions of low energy are believed to have their angular distributions attenuated by extra nuclear effects and these are shown with dotted error bars. Some points with very large errors have been omitted from this plot.

Fig. 9. Partial level scheme for ^{186}Os, showing some of the transitions which we observed in the reaction ^{184}W(^{4}He,2n)^{186}Os. Relative transition intensities, corrected for internal conversion, are shown in brackets. Other strong transitions, not shown in this figure, were also seen.

References

1) H. Morinaga and P. C. Gugelot, Nuclear Physics 46 (1963) 210

2) F. S. Stephens, N. L. Lark and R. M. Diamond, Nuclear Physics 63 (1964) 82

3) N. L. Lark and H. Morinaga, Nuclear Physics 67 (1965) 315

4) M. Sakai, T. Yamazaki and H. Ejiri, Nuclear Physics 74 (1965) 81

5) J. Burde, R. M. Diamond and F. S. Stephens, to be published

6) N. L. Lark, J. O. Newton and F. S. Stephens, to be published

7) J. O. Newton, M. J. Emmott, J. R. Leigh and D. Ward, to be published

8) H. Ejiri, M. Ishihara, M. Sakai, K. Katori and T. Inamura, Phys. Letters 18 (1965) 314; H. Ejiri, M. Ishihara, M. Sakai, T Inamura and K. Katori, J. Phys. Soc. Japan 21 (1966) 1

9) R. M. Diamond, E. Matthias, J. O. Newton and F. S. Stephens, Phys. Rev. Letters 20 (1966) 56

10) I. M. Band, M. A. Listengarten, L. A. Sliv and J. E. Thun, Alpha, Beta and Gamma Ray Spectroscopy Vol 2 (1965) 1683, ed by K. Seigbahn, N. Holland Pub. Co.

11) M. E. Rose, L. C. Biedenharn, and G. Arfken, Phys. Rev. 85 (1952) 5

12) R. M. Diamond and F. S. Stephens, Nuclear Physics 45 (1963) 632

13) M. J. L. Yates, Alpha, Beta and Gamma Ray Spectroscopy, Vol 2 (1965) 1691, ed. by K. Seigbahn, North Holland Pub. Co.

14) J. O. Newton, F. S. Stephens and R. M. Diamond, Nuclear Physics (1967)

15) A. J. Haverfield, F. M. Bernthal and J. M. Hollander, UCRL 16862 (to be published in Nuclear Physics)

16) A. Williams, Nuclear Physics 52 (1964) 324

17) J. E. Monahan, S. Raboy and C. C. Trail, Phys. Rev. 123 (1961) 1373

18) L. A. Sliv and I. M. Band, Alpha, Beta and Gamma Ray Spectroscopy, Vol 2 (1965) 1639, ed. by K. Seigbahn, North Holland Pub. Co.

19) J. M. Alexander and G. N. Simonoff, Phys. Rev. 133 (1963) B93

20) J. D. Jackson, Can. J. Phys. 34 (1956) 767

21) L. C. Biedenharn, "Angular Correlations", Nuclear Spectroscopy, ed. by F. Ajzenberg-Selove (American Press, New York, 1960) Chap. V

22) J. F. Mollenauer, Phys. Rev. 127 (1962) 867

23) J. R. Grover, Phys. Rev 127 (1962) 2142

24) T. Sikkeland and V. E. Viola, Proc. 3rd Conf. on Reactions between Complex Nuclei, Asilomar (1963) 232 (University of California Press, Berkeley)

25) T. Sikkeland, Phys. Rev. 135 (1964) B669

26) G. A. Pik-Pichak, JETP 38 (1960) 768

27) T. D. Thomas, Nucl. Phys. 53 (1964) 577

28) D. Sperber, Phys. Rev. 142 (1966) 578

29) J. O. Rasmussen and T. T. Sugihara, Phys. Rev. to be published

30) H. Frauenfelder and R. M. Steffen, Alpha, Beta and Gamma Ray Spectroscopy, Vol. 2 (1965) 997, ed. by K. Seigbahn, North Holland Pub. Co.

31) G. T. Emery, W. R. Kane, M. McKeown, M. L. Perlman and G. Scharff-Goldhaber, Phys. Rev. 129 (1963) 2597

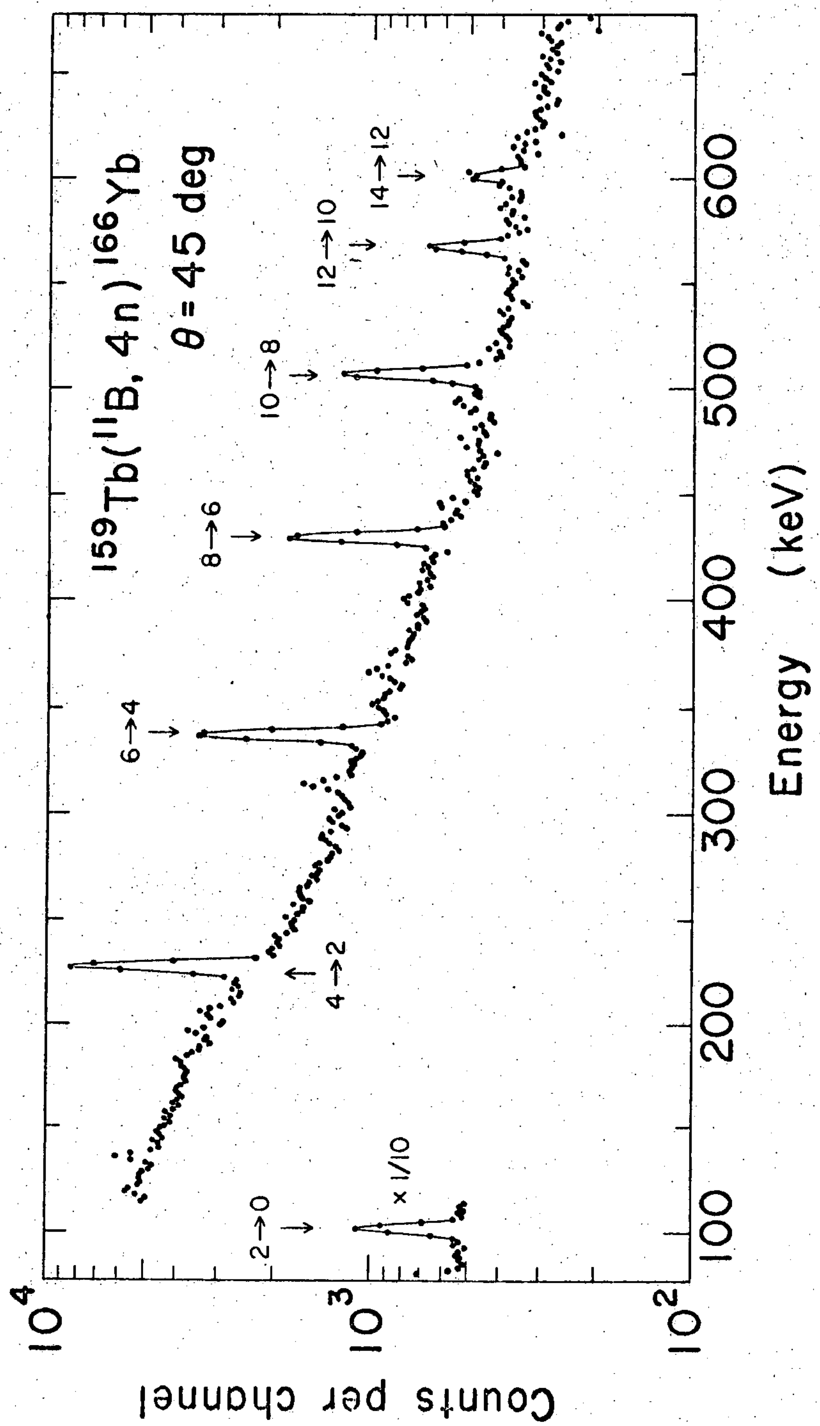

MUB 13603

Fig. 1 a

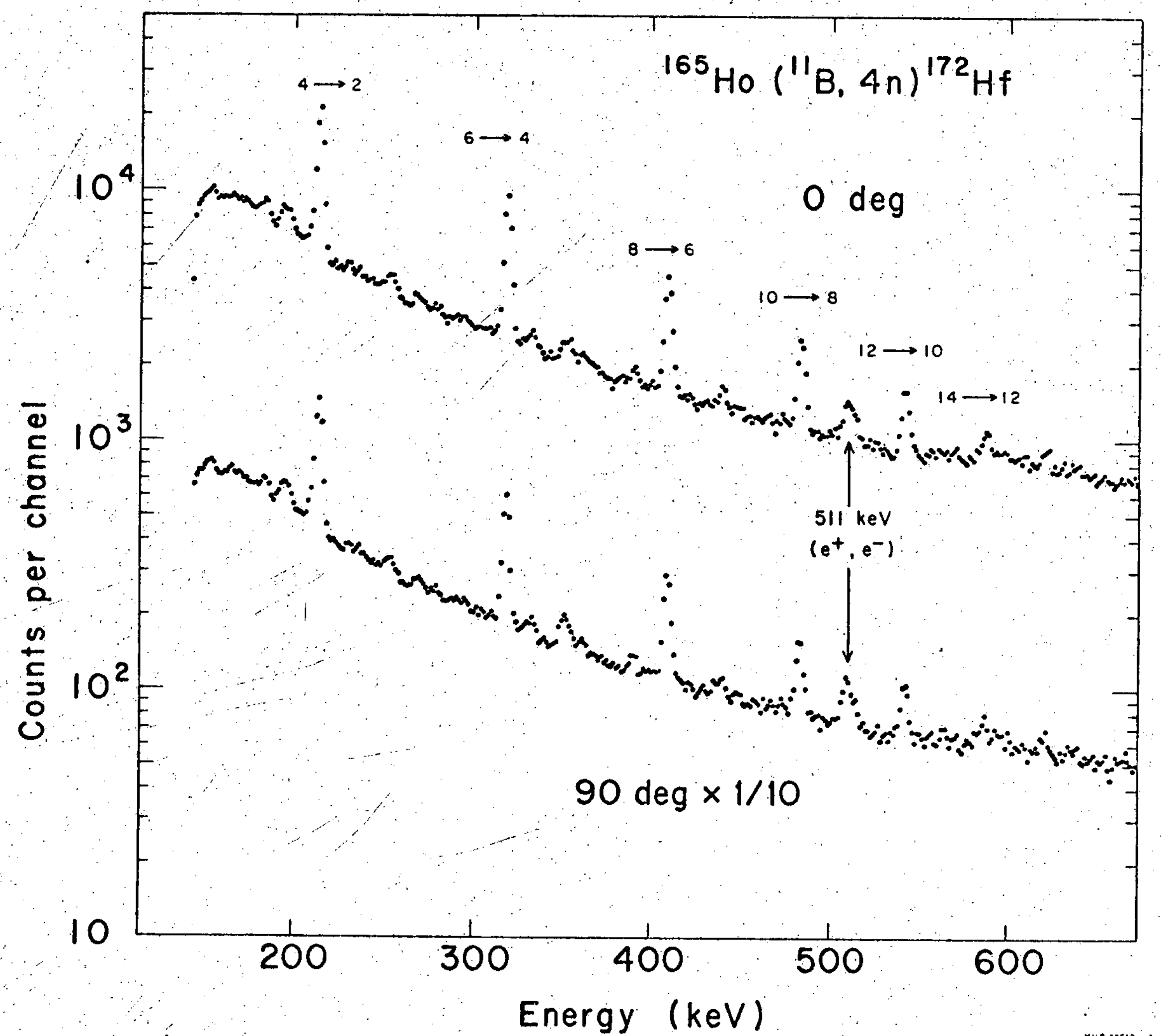

^{165}Ho (^{11}B, 4n)^{172}Hf
0 deg
90 deg × 1/10
4 ⟶ 2
6 ⟶ 4
8 ⟶ 6
10 ⟶ 8
12 ⟶ 10
14 ⟶ 12
511 keV
(e+, e−)
Counts per channel
Energy (keV)
10
10²
10³
10⁴
200
300
400
500
600

Fig. 1b

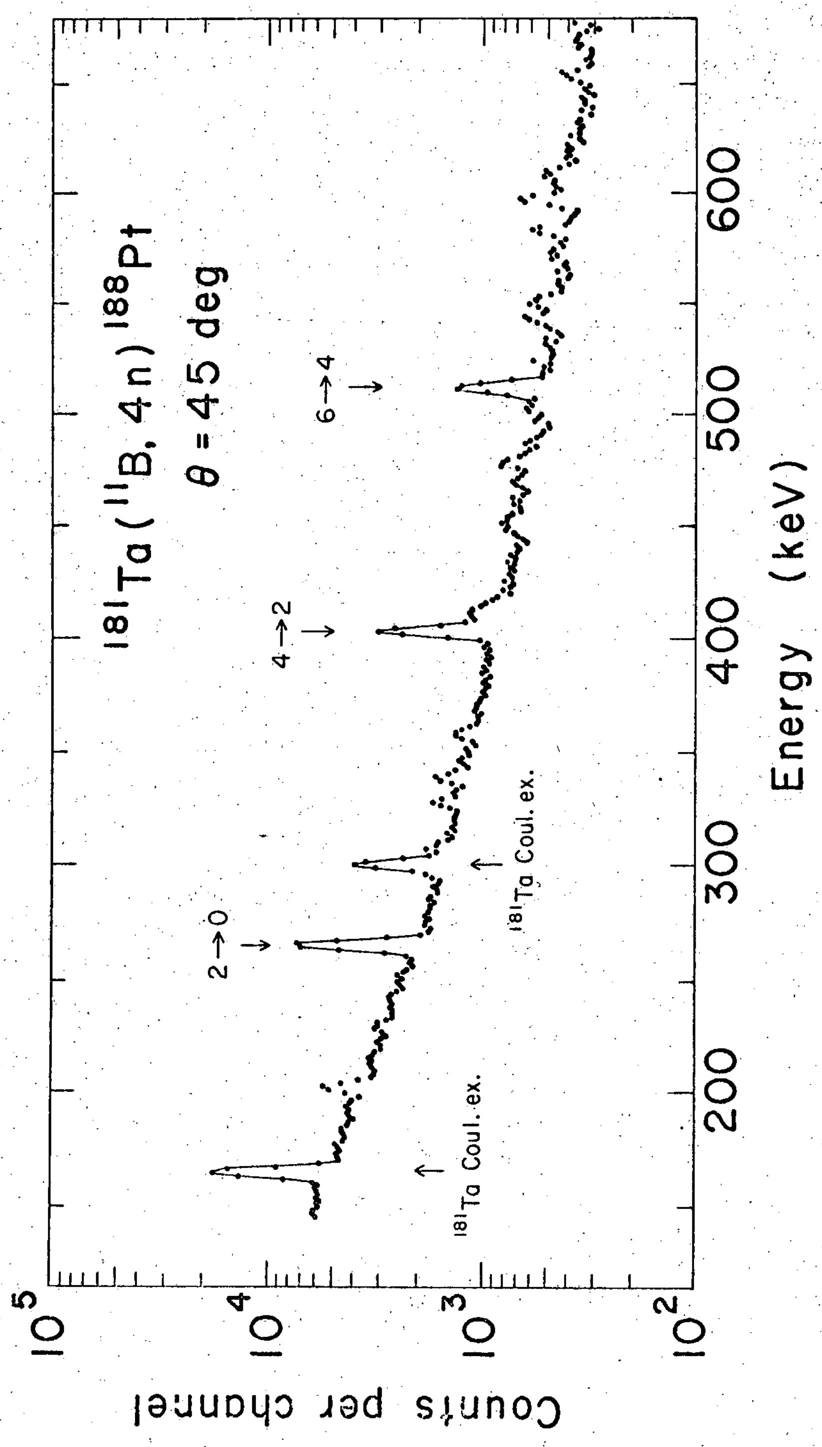

MUB-13595

Fig. 1c

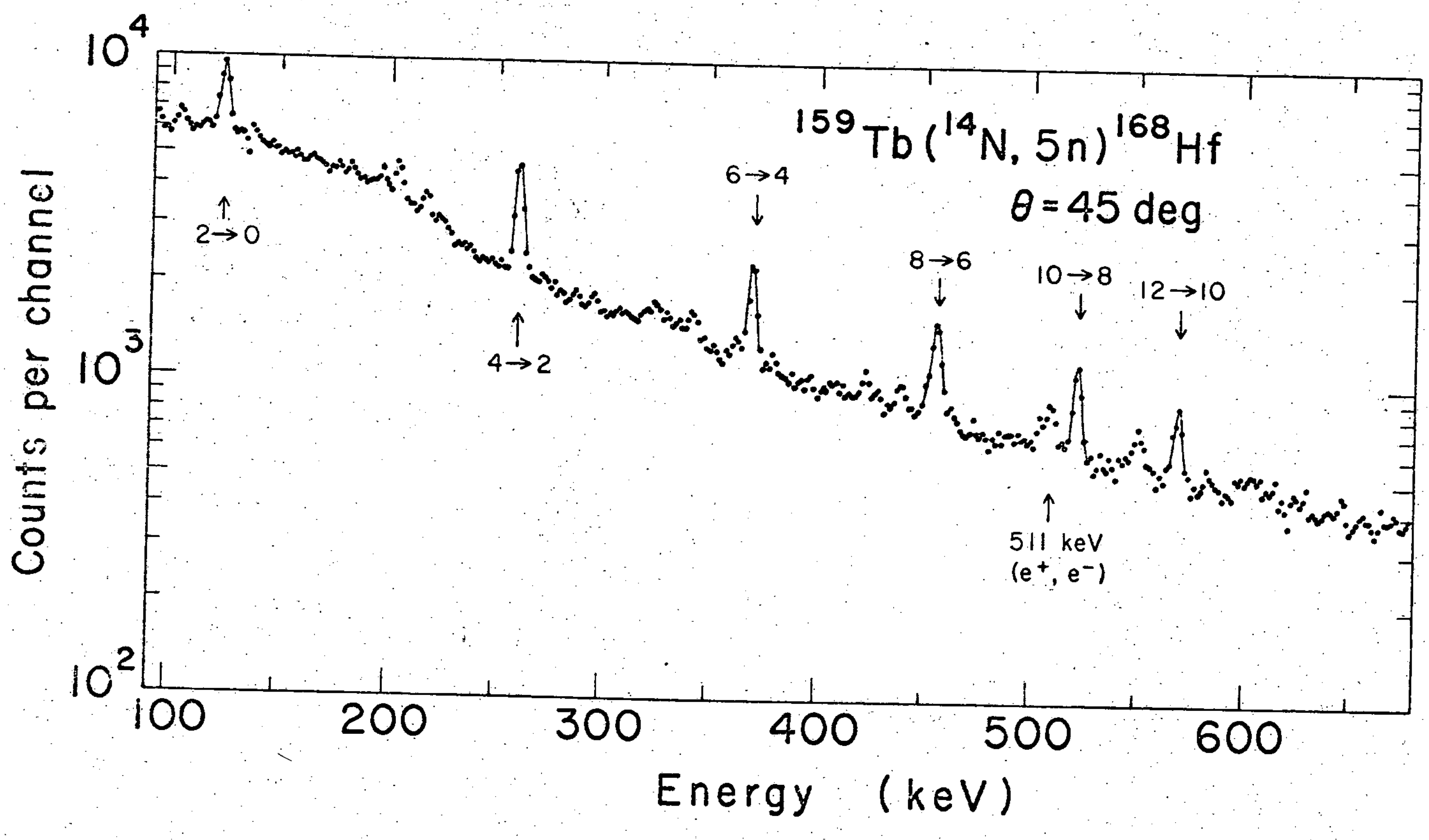

$^{159}Tb(^{14}N, 5n)^{168}Hf$
$\theta = 45$ deg
2→0
4→2
6→4
8→6
10→8
12→10
511 keV
(e^+, e^-)
Counts per channel
10^4
10^3
10^2
100
200
300
400
500
600
Energy (keV)
MUB-13604

Fig. 2a

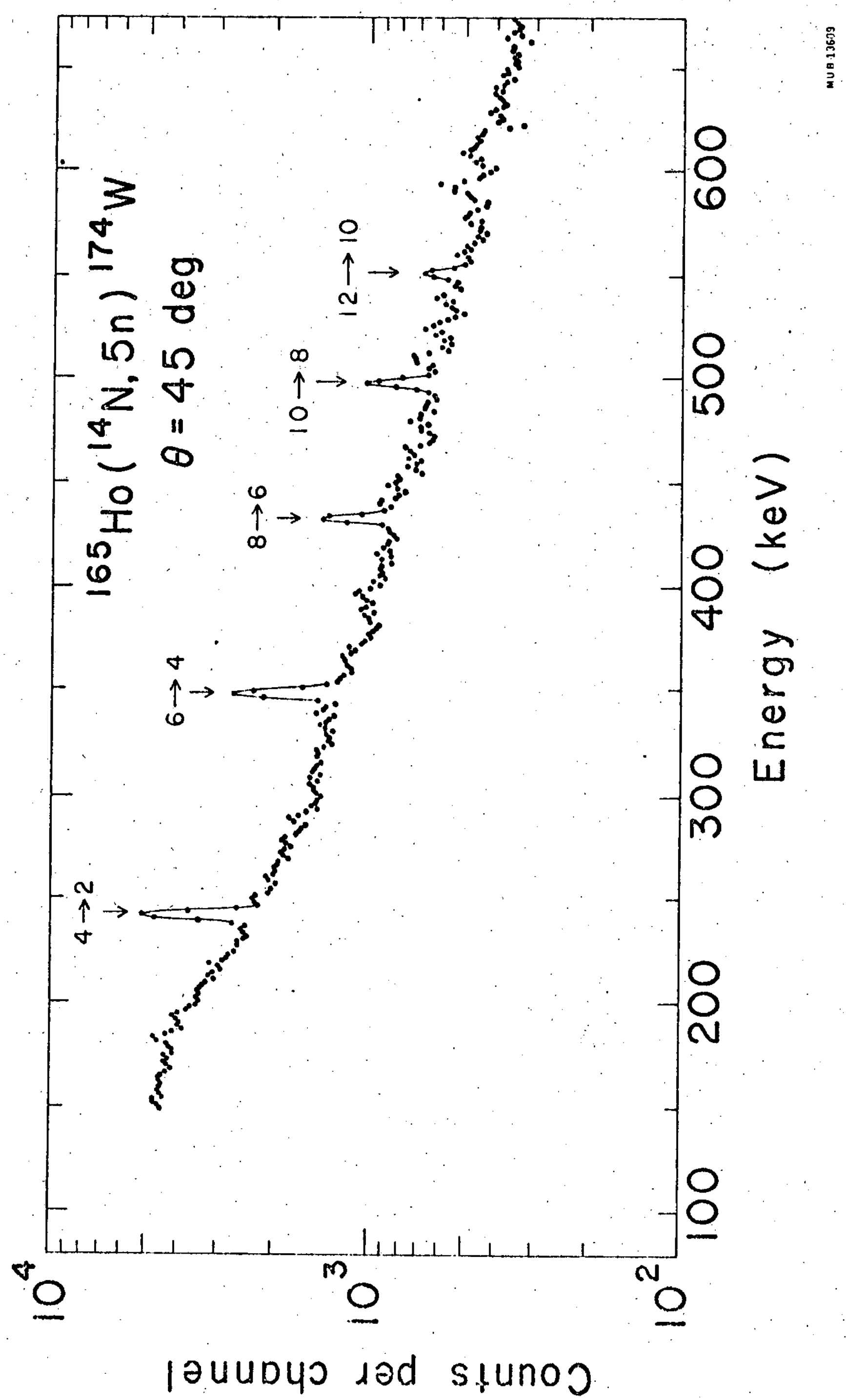

^{165}Ho(^{14}N,5n)^{174}W
θ = 45 deg
4→2
6→4
8→6
10→8
12→10
100
200
300
400
500
600
Energy (keV)
10^4
10^3
10^2
Counts per channel
MUB 13609

Fig. 2b

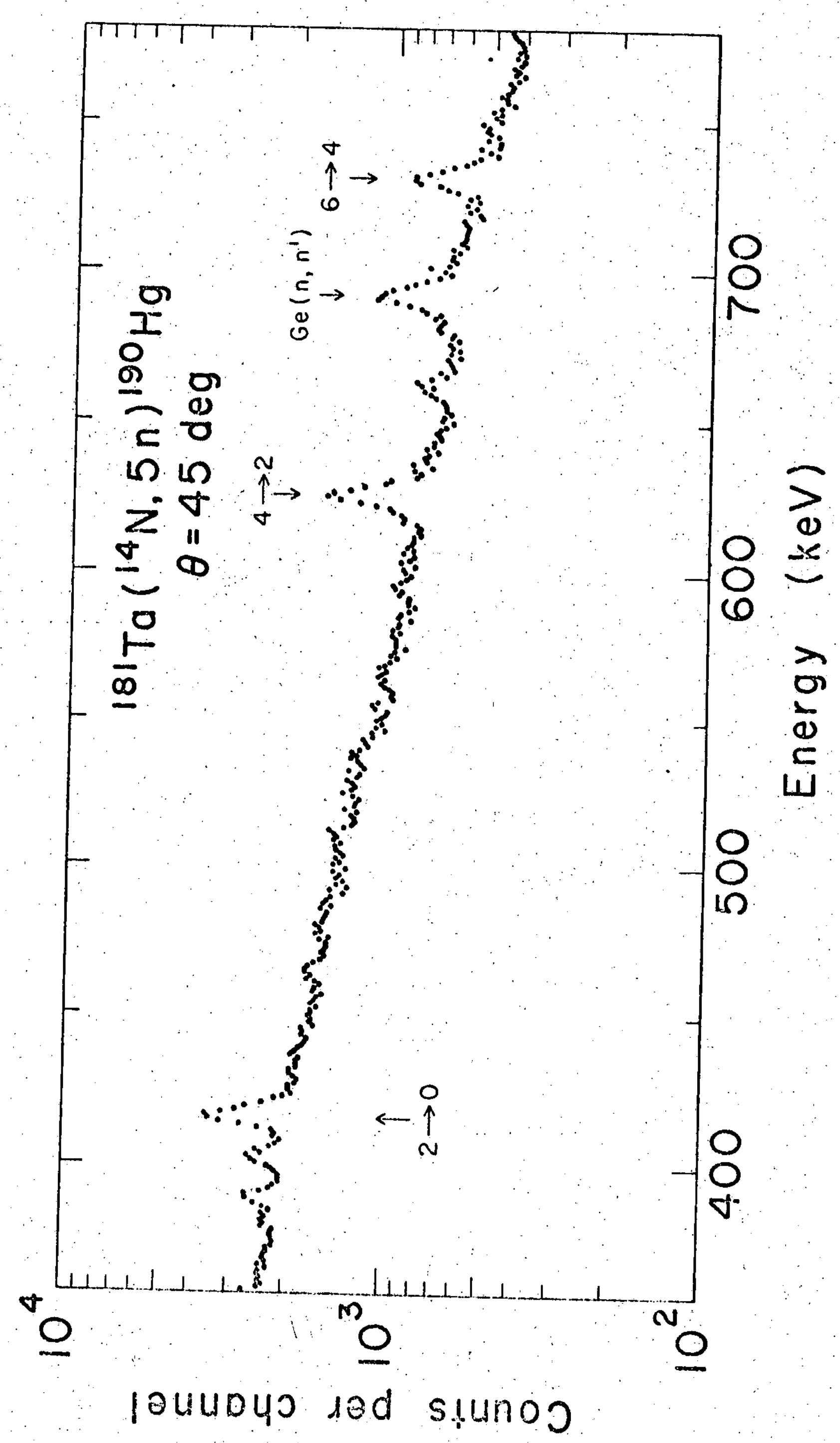

MUB13605

Fig. 2c

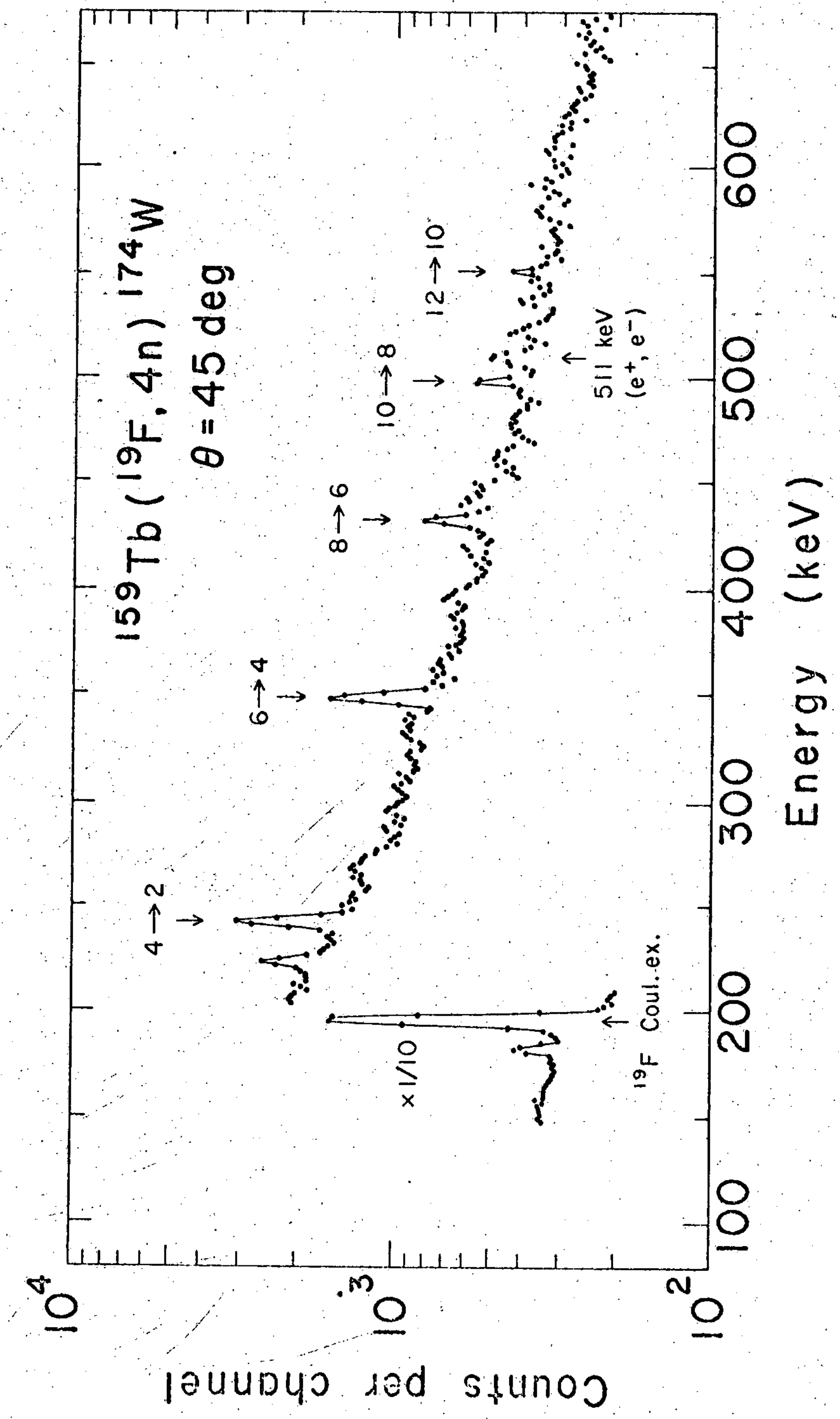

MUB 13606

Fig. 3

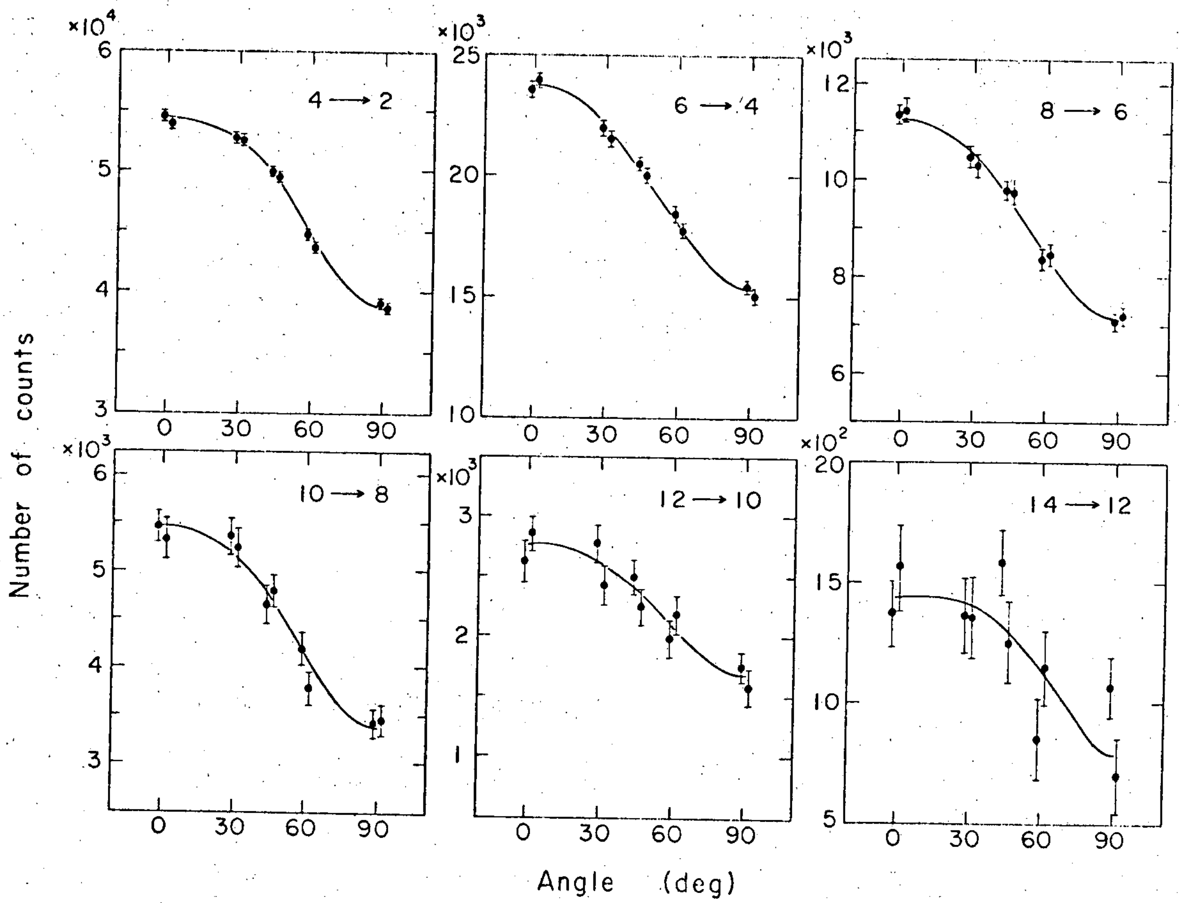

×10⁴
6
5
4
3
4 → 2
0 30 60 90
×10³
25
20
15
10
6 → 4
0 30 60 90
×10³
12
10
8
6
8 → 6
0 30 60 90
Number of counts
×10³
6
5
4
3
10 → 8
0 30 60 90
×10³
3
2
1
12 → 10
0 30 60 90
×10²
20
15
10
5
14 → 12
0 30 60 90
Angle (deg)

Fig. 4

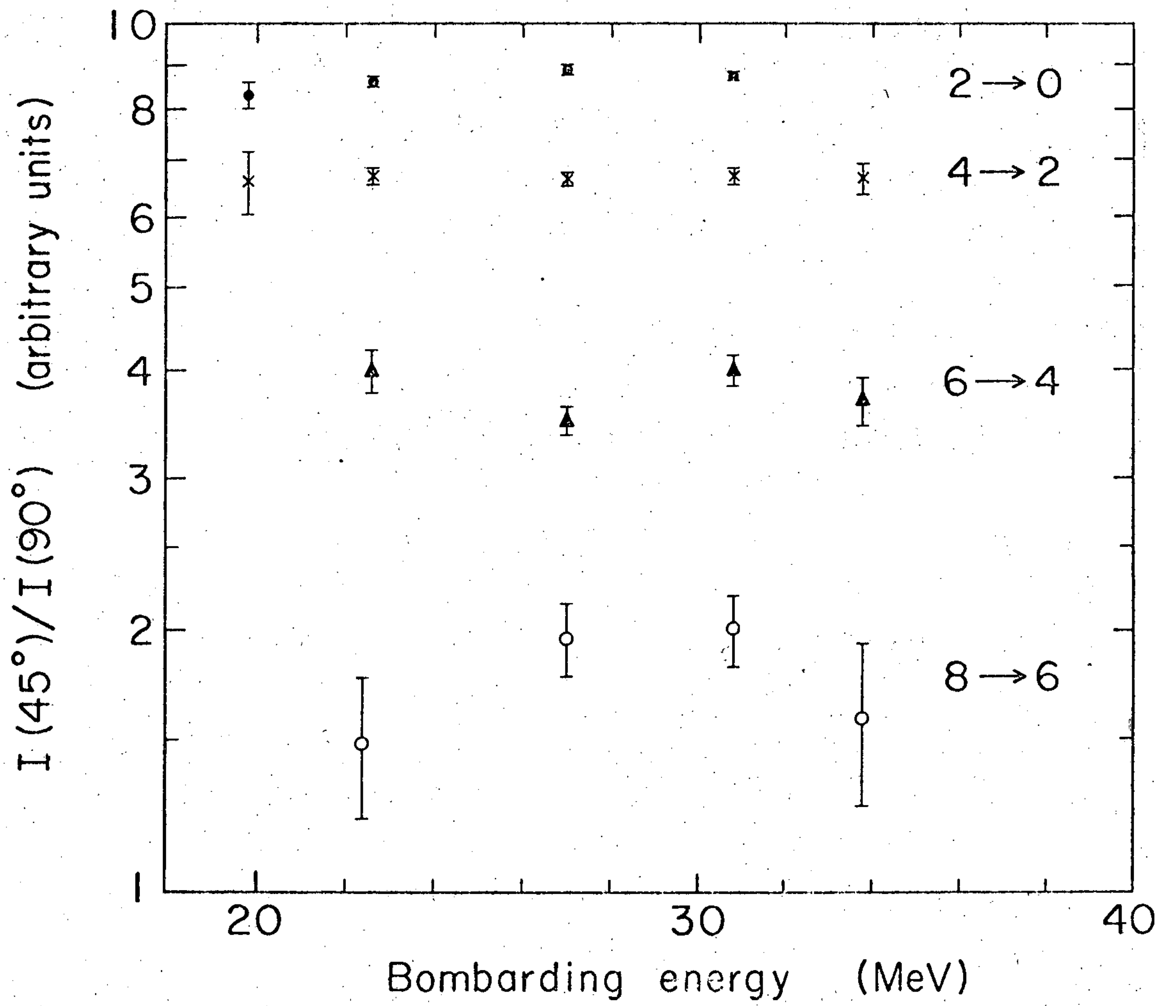

Fig. 5

MUB-13596

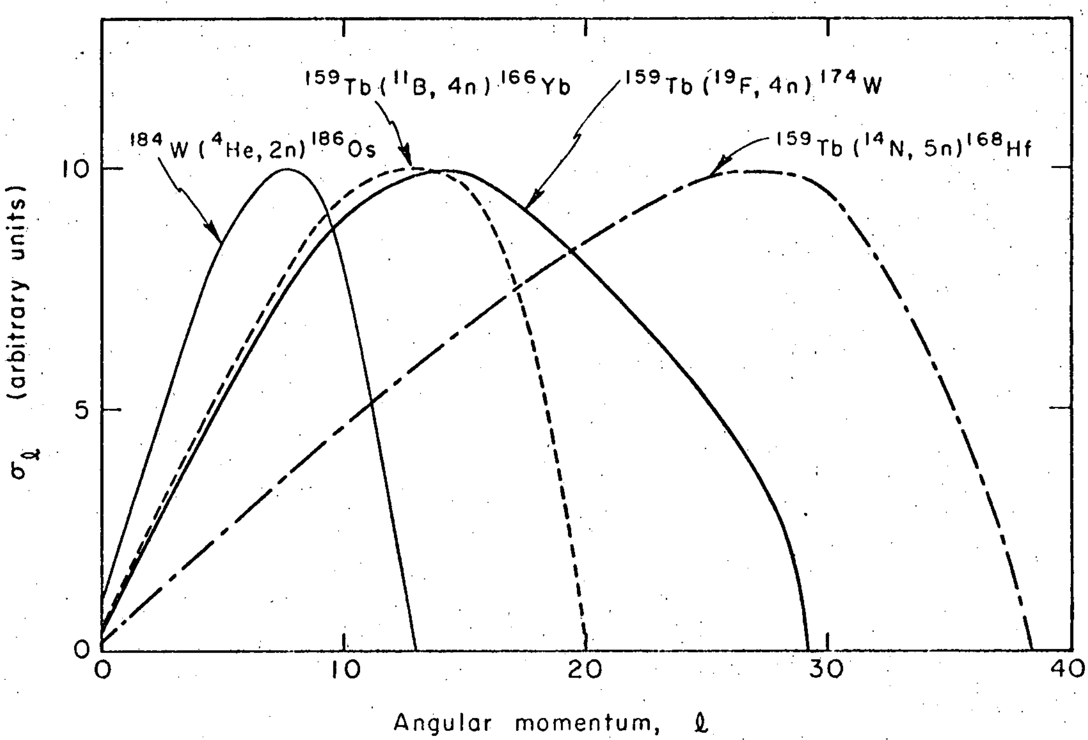

Fig. 6

MUB-13597

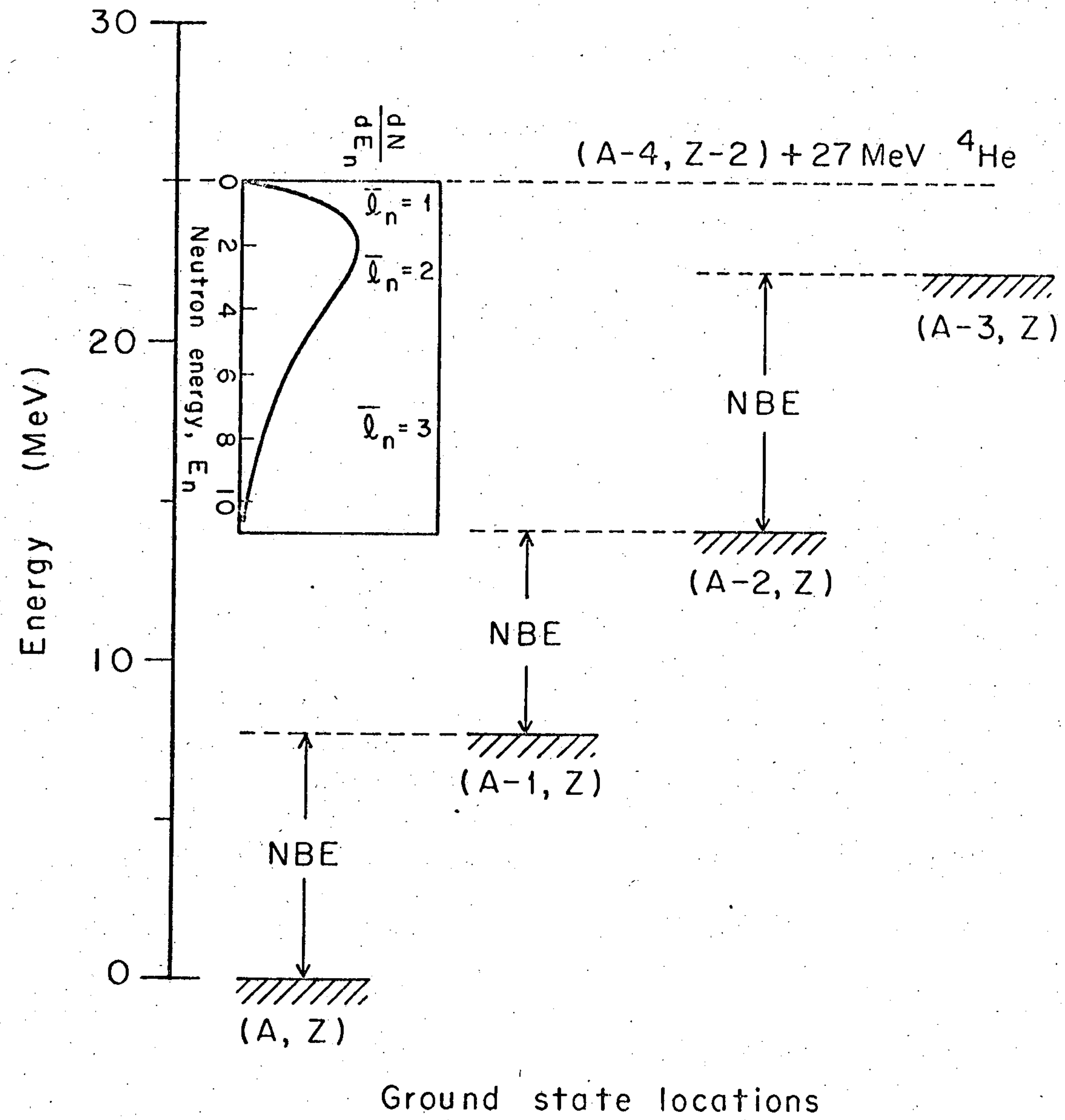

Fig. 7

MUB 13593

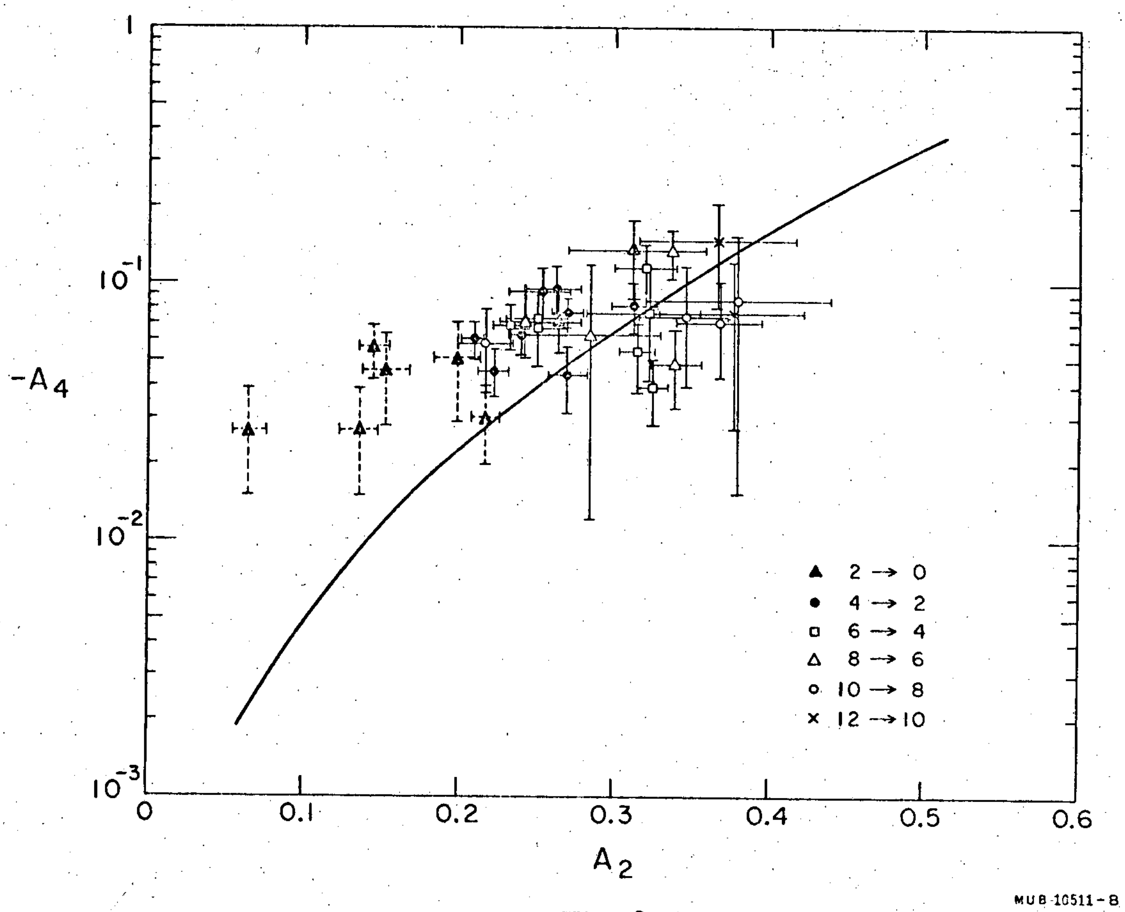
1
10^{-1}
10^{-2}
10^{-3}
$-A_4$
0
0.1
0.2
0.3
0.4
0.5
0.6
A_2
2 → 0
4 → 2
6 → 4
8 → 6
10 → 8
12 → 10
MUB-10511-B

Fig. 8

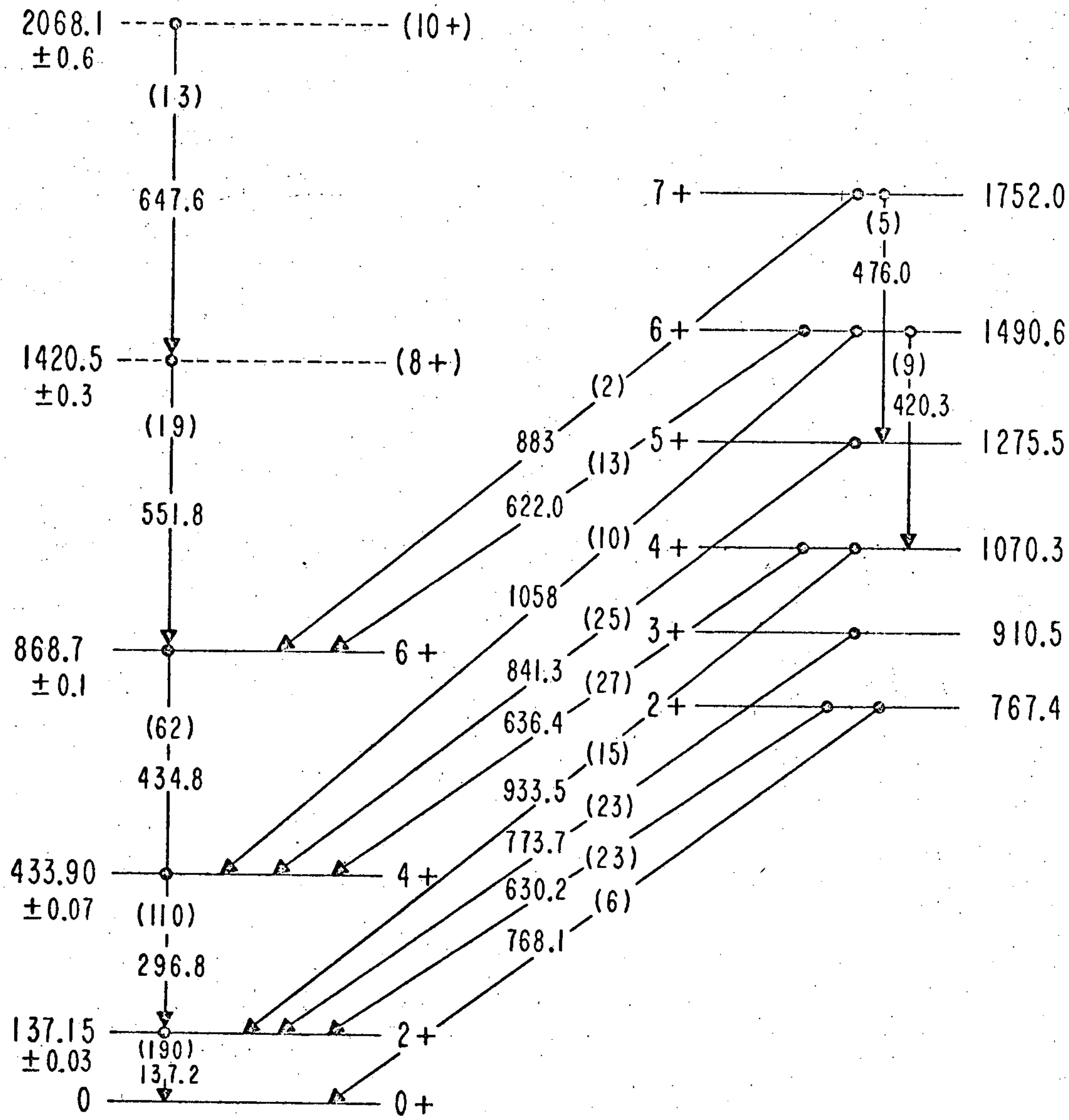

2068.1
±0.6
(10+)
(13)
647.6
7+
1752.0
(5)
476.0
6+
1490.6
(9)
420.3
1420.5
±0.3
(8+)
(19)
(2)
883
(13)
622.0
5+
1275.5
551.8
(10)
1058
4+
1070.3
(25)
3+
910.5
868.7
±0.1
6+
841.3
(27)
636.4
2+
767.4
(62)
434.8
(15)
933.5
(23)
773.7
(23)
630.2
(6)
768.1
433.90
±0.07
4+
(110)
296.8
137.15
±0.03
2+
(190)
137.2
0
0+
MUB-13598

^{186}Os

Fig. 9